CORE
Metadata, citation and similar papers at core.ac.uk
Provided by Elsevier - Publisher Connector

Available online at www.sciencedirect.com
ScienceDirect
St. Petersburg Polytechnical University Journal: Physics and Mathematics 2 (2016) 41–49
www.elsevier.com/locate/spjpm

Crystal acceleration effect for cold neutrons in the vicinity of the Bragg resonance

Yulia P. Braginetz[a,b,*], Yaroslav A. Berdnikov[a], Valery V. Fedorov[a,b], Igor A. Kuznetsov[b], Mikhail V. Lasitsa[a,b], Sergey Yu. Semenikhin[b,*], Egor O. Vezhlev[a,b], Vladimir V. Voronin[a,b]

[a] *Peter the Great St. Petersburg Polytechnic University, 29 Politekhnicheskaya St., St. Petersburg 195251, Russian Federation*
[b] *Petersburg Nuclear Physics Institute, Orlova Roscha, Gatchina 188300, Leningrad Oblast, Russian Federation*

Available online 4 March 2016

Abstract

A new mechanism of neutron acceleration is studied experimentally in detail for cold neutrons passing through the accelerated perfect crystal with the energies close to the Bragg one. The effect arises due to the following reason. The crystal refraction index (neutron–crystal interaction potential) for neutron in the vicinity of the Bragg resonance sharply depends on the parameter of deviation from the exact Bragg condition, i.e. on the crystal–neutron relative velocity. Therefore the neutrons enter into the accelerated crystal with one neutron–crystal interaction potential and exit with the other. Neutron kinetic energy cannot vary inside the crystal due to its homogeneity. So, after passage through such a crystal, neutrons will be accelerated or decelerated because of the different energy change at the entrance and exit crystal boundaries.

Copyright © 2016, St. Petersburg Polytechnic University. Production and hosting by Elsevier B.V.
This is an open access article under the CC BY-NC-ND license (http://creativecommons.org/licenses/by-nc-nd/4.0/).

Keywords: Neutron acceleration; Perfect crystal; Neutron diffraction; Accelerated crystal.

1. Introduction

The possibility of controlling the energy of neutron beams is of great interest because of the wide neutron applications in various scientific fields from material science to nuclear physics, particle physics and astrophysics. The acceleration effect for neutrons scattered by excited isomeric nuclei was first predicted in 1959 [1] and was discovered experimentally in 1980 [2,3]. The acceleration of neutrons in an inversely populated medium [4,5] turned out to be very important in processes of stellar nucleosynthesis. In Ref. [6] acceleration of neutrons by vibrationally excited nitrogen molecules was observed.

Acceleration of neutrons in the uniform magnetic field by means of a radio-frequency flipper is well known and successfully used in physical experiments (see, e.g., Ref. [7]). The phenomenon of neutron acceleration in a strong alternating magnetic field (of amplitude ~0.4 T) was observed in Ref. [8]. The acceleration of neutrons in a weak alternating magnetic

* Corresponding author.
E-mail addresses: aiver@pnpi.spb.ru (Yu.P. Braginetz), berdnikov@spbstu.ru (Ya.A. Berdnikov), vfedorov@pnpi.spb.ru (V.V. Fedorov), ikuz@pnpi.spb.ru (I.A. Kuznetsov), mishlas1@gmail.com (M.V. Lasitsa), ssy@pnpi.spb.ru (S.Yu. Semenikhin), evezhlev@gmail.com (E.O. Vezhlev), vvv@pnpi.spb.ru (V.V. Voronin).

http://dx.doi.org/10.1016/j.spjpm.2016.02.007
2405-7223/Copyright © 2016, St. Petersburg Polytechnic University. Production and hosting by Elsevier B.V. This is an open access article under the CC BY-NC-ND license (http://creativecommons.org/licenses/by-nc-nd/4.0/).
(Peer review under responsibility of St. Petersburg Polytechnic University).

field (of 0.1–1.0 mT) was measured using anomalous behaviour of the velocity dispersion for neutrons, moving in a crystal close to the Bragg directions [9]. The foundations of the neutron acceleration in a laser radiation field were considered in Ref. [10].

Also acceleration and deceleration of neutrons by reflection from moving mirror [11,12] or by Doppler-shifted Bragg diffraction from a moving crystal [13,14] are well-known and used in experiments with ultracold neutrons.

Recently a new interest has arisen in the acceleration of neutrons passing through accelerating media [15,16]. This effect was first observed by the authors of Ref. [17] and was described in detail in Ref. [18]. It was noted in Ref. [18] that "the observed effect was a manifestation of quite a general phenomenon – the accelerated medium effect (AME) inherent to waves and particles of different nature". In Ref. [19], the acceleration and deceleration of neutrons were observed by applying a specific time-of-flight method. In Ref. [20], some new special features of the effect for a birefringent medium were discussed with the applications to neutron spin optics and evolution of flavor states of neutrino, propagating through a free space. The acceleration of the samples in the mentioned experiments reached several tens of g units, and the value of the energy transfer ΔE_n to a neutron with energy E_n

$$(\Delta E_n \approx 2(\Delta v/v_n)E_n[(1 - -n)/n])$$

fell within the range of $(2–6)\cdot 10^{-10}$ eV [18] for ultracold neutrons (UCN), so up to now AME was observed only for UCN and by only one research group (see Refs. [18,20]). Here v_n is a neutron velocity, Δv is a value of a relative neutron-matter velocity variation during the neutron time-of-flight through the sample, n is the refraction index for neutron.

In the present paper, a new much more effective mechanism of acceleration effect is proposed [21], which has been tested and confirmed experimentally for cold neutrons passing through the accelerated perfect crystal. An energy transfer to a neutron in this case can be at the level of $\sim 4\cdot 10^{-8}$ eV. This value in contrast to AME is determined by the amplitude V_g of the corresponding harmonic of the nuclear neutron–crystal periodic potential, but not by the value of a relative neutron–crystal velocity variation during the neutron time-of-flight through the crystal. For cold neutron

$$[(1 - n)/n] \approx V_0/2E_n,$$

so AME in our case has an order

$$\Delta E_n \approx (\Delta v/v_n)V_0 \sim 10^{-5}, V_0 \sim 10^{-13}\text{eV}$$

that is negligible in further consideration (V_0 is zero harmonic of neutron–crystal interaction potential, i.e. averaged crystal potential).

The essence of the crystal acceleration effect is as follows. The crystal refraction index for neutrons in the vicinity of the Bragg resonance sharply depends on the crystal–neutron relative velocity (see further). The neutrons enter into accelerated crystal with one potential of a neutron–crystal interaction and exit with the other potential, so the kinetic energy change at the crystal boundaries will differ, and neutrons will be accelerated or decelerated after passage trough such a crystal, in this case the energy transfer to a neutron being at the level of $\sim 4\cdot 10^{-8}$ eV.

Neutron wave function significantly modifies for neutrons moving through the crystal under conditions close to the Bragg ones. As a result neutrons concentrate on "nuclear" planes or between them [22,23]. We take the term "nuclear" planes to mean the positions of maxima of periodic nuclear potential for corresponding system of crystallographic planes. The neutron–crystal interaction potential can be written as a sum (the reciprocal lattice vectors expansion) of harmonic potentials (harmonics) corresponding to all nuclear plane systems described by reciprocal lattice vector $\mathbf{g}$ normal to the given plane system, $|\mathbf{g}|=2\pi/d$(d is an interplanar distance):

$$V(\mathbf{r}) = \sum_g V_g e^{i\mathbf{gr}} = V_0 + \sum_{g>0} 2v_g \cos(\mathbf{gr} + \varphi_g). \qquad (1)$$

Here V_g are the amplitudes of g-harmonics of the crystal nuclear potential, which are determined by neutron scattering amplitudes for crystal elementary cell (structural amplitudes). In general, V_g are complex values, i.e. $V_g = v_g \exp\varphi_g$.

However, if the crystal is nonabsorbing and centrosymmetric, all phases can be turned to zero at once, i.e. all V_g can be made real, by putting the coordinate origin at the centre of symmetry. When a neutron is moving through the crystal under conditions close to the Bragg ones for a plane system $\mathbf{g}$, only one harmonic with amplitude V_g will be essential and should be taken into account. That is due to a very narrow wavelength width for Bragg reflection of neutrons. For one harmonic, the origin of coordinates can be always placed at its maximum making the V_g amplitude real. Just the same can be done with the crystal electric potential. So for centrosymmetric crystals the positions of "nuclear" and "electric" planes always coincide.

But if the center of symmetry is absent, the maxima of electric potential for some crystallographic planes will be shifted relative to the nuclear maxima. That

will lead to gigantic electric fields, acting on the neutron inside the crystal [23–25], because the neutrons concentrate in the vicinities of the maxima and minima of nuclear potential where electric field is just nonzero in this case. So the whole class of new neutron optics phenomena arises (see, for example, Ref. [26]).

2. Neutron crystal optics

Interest in neutron optics in the perfect crystals has accelerated in the past few years. It is caused first by new outstanding possibilities for studies of neutron fundamental properties and its interactions. A case in point is, for instance, a search for a neutron electric dipole moment, as well as a search for CP-violating pseudomagnetic forces due to exchange of a pseudoscalar axion-like particle, using neutron optics in crystal [27–32]; these are now the most important tasks.

The admixture of the waves reflected by crystallographic planes to the neutron wave function significantly changes the pattern of neutron propagation in the crystal and leads to new phenomena, which manifest sharply defined resonance character with Bragg (Darvin) width. For example, a small change of the neutron energy within this width ($\Delta E/E \sim 10^{-5}$ for thermal and cold neutrons) results in significant changing the neutron mean velocity in crystal (the anomalous velocity dispersion), and so the sharp energy dependence of the neutron-traveltime through the crystal on neutron energy exhibits [33].

In the present paper we discuss one more phenomenon related to the change in the neutron wave function in the crystal, namely the resonant behavior of neutron refractive index (i.e. kinetic energy of neutron inside the crystal) depending on the difference of the initial and Bragg neutron energies. If a neutron passes through the non-absorbing perfect crystal and Bragg conditions are not satisfied for any crystallographic planes, the neutron propagation through the crystal can be described by the refractive index which depends on the V_0 amplitude of zero harmonic (average crystal potential). In this paper, a perfect crystal means a crystal with the dispersion of the interplanar distance much less than the intrinsic width of the Bragg reflection. But when the energy or velocity direction of a neutron approaches the Bragg values, the waves reflected by the corresponding plane system start arising. The amplitudes of these waves are determined by the corresponding V_g amplitudes ofpotential harmonics and by the deviations from the exact Bragg condition. When this deviation being more than the harmonic amplitude we can use the perturbation theory [28,34]. In this case if the neutron has an initial energy equal to E_0 and the wave vector $\mathbf{k}_0$ ($E_0 = \hbar \mathbf{k}_0/2m$), its wave function inside the crystal will be written as

$$\psi = e^{i\mathbf{kr}} + \frac{V_g}{E_k - E_{k_g}} e^{i\mathbf{k_g r}} \equiv e^{i\mathbf{kr}}\left[1 - \frac{1}{\Delta_B} e^{i\mathbf{gr}}\right], \qquad (2)$$

where

$$\Delta_B = (E_k - E_{k_g})/V_g = 2(E_k - E_B)/V_g$$

is the dimensionless parameter of deviation from the exact Bragg condition for some $\mathbf{g}$ system of planes; $\mathbf{k},\mathbf{k}_g = \mathbf{k}+\mathbf{g}$ are the wave vectors of incident and reflected waves inside the crystal with the mean refraction index taken into account; E_k and E_{k_g} are the unperturbed neutron kinetic energies in states $|\mathbf{k}\rangle$ and $|\mathbf{k_g}\rangle$,

$$E_k = \hbar^2 k^2/2m = \hbar^2 k_0^2/2m - V_0,$$

$$E_{k_g} = \hbar^2 k_g^2/2m$$

$$E_B = \hbar^2 g^2/(8m \sin^2\theta_B)$$

is the neutron energy that corresponds to exact Bragg condition. The presence of a reflected wave with the amplitude equal to $1/\Delta_B$ leads to localization of neutron density in crystal on(or between) reflecting planes depending on the sign of Δ_B:

$$|\psi(\mathbf{r})|^2 = 1 - \frac{2}{\Delta_B}\cos(\mathbf{gr}). \qquad (3)$$

The concentration of neutron density in the vicinity of maxima or minima of nuclear potential, as in the case of Laue diffraction, leads to additional changing the neutron kinetic energy $\tilde{E}_k$ and, respectively, the value of wave vector and refractive index n inside the crystal depending on the magnitude of this concentration, i.e. on deviation parameter $\Delta_B$from the Bragg condition. Notice that the neutron refraction index n is determined as usual:

$$n^2 = 1 - \tilde{E}_k/E_0.$$

Averaging the potential over the wave function (2), using (3), one gets

$$\tilde{E}_k = \frac{\hbar^2 \tilde{k}^2}{2m} = E_0 - V_0 + V_g \cdot \frac{1}{\Delta_B}. \qquad (4)$$

The last term in Eq. (4) increases infinitely approaching the Bragg condition ($E_k = E_{k_g}$), so it becomes incorrect (and the perturbation theory is inapplicable as well) already for

$$E_k - E_{k_g} \sim V_g.$$

The precise fulfilment of the Bragg condition

$$E_k - E_{k_g} = 0$$

means the equality of energies for two neutron states with momenta $\hbar\mathbf{k}$ and $\hbar(\mathbf{k}+\mathbf{g})$, i.e. the neutron energy level E_k becomes doubly degenerated. Amplitudes of these neutron states become comparable in value, and one should solve well-known two-level problem that corresponds to the two-wave approximation of the dynamic diffraction theory. Result is the following. Neutrons with the energies within the Bragg (Darwin) width $|E_k - E_B| \leq V_g/2$ cannot penetrate into the working K_3 crystal (Fig. 1), they will completely reflect from the crystal entrance face which is parallel to the crystallographic planes. So only the neutrons with $|E_k - E_B| > V_g/2$ ($\Delta_B > 1$) can pass through this crystal and can be accelerated. Using the expansion of the exact two wave dispersion equation over $1/\Delta_B$, the following result for the kinetic energy of the neutron after its entrance into the crystal can be obtained:

$$\tilde{E}_k = E_0 - V_0 + V_g \cdot \frac{\Delta_B}{\Delta_B^2 + 1}. \quad (5)$$

The last term in Eq. (5) describes the additional potential neutron energy due to neutron localization. It significantly changes with small variation of neutron energy within the Bragg reflection width $\Delta_B \cong 1$, i.e. in the narrow energy range

$$E_B - V_g < E_k < E_B + V_g.$$

For thermal and cold neutrons $V_g/E_B \cong 10^{-5}$. The V_g amplitude value itself is comparable to that of the mean crystal potential V_0. Hence, by changing the incident neutron energy in the vicinity of E_B, a well-defined resonance-type energy dependence of the neutron refraction index can be observed in the crystal. For example, for (110) plane of quartz $V_g = 4\cdot10^{-8}$ eV, $V_0 = 10^{-7}$ eV, and $E_B = 3.2\cdot10^{-3}$ eV for a diffraction angle close to $\pi/2$.

It is worth to notice that in our case Eq. (4) can also be quite a good approximation, the infinities can be removed by overaging over the neutron spectrum within $\Delta_B \sim 2$, because it is formed by two crystals K_1 and K_2. When $\Delta_B = 0$ for the central part of the spectrum only the left and the right wings, having opposite potentials connected with the neutron concentration, can penetrate to the crystal so that averaged potential for this neutrons will be zero in accordance with Eq. (5).

3. Experimental setup

Our experiment was carried out at the horizontal neutron beam of the WWR-M reactor (PNPI, Gatchina, Leningrad Region, Russia). The energy change of a neutron passed through the accelerating crystal near to the Bragg condition was measured.

If the neutron moves through the accelerating crystal, then the parameter of deviation from the Bragg condition and correspondingly the mean potential of neutron–crystal interaction will be time-dependent (see Eq. (5)). As a result, the refractive index will vary during a neutron travel in the crystal. Correspondingly, the changes in the neutron kinetic energies at the entrance and the exit surfaces of the crystal will differ. Therefore, one should observe either acceleration or deceleration of the neutron passing through such a crystal, because the kinetic energy $\tilde{E}_k$ of the neutron inside the crystal does not change because of the crystal homogeneity. It should be noticed that it does not matter in which way a change in the parameter of deviation from the Bragg condition occurs over a time interval of the neutron propagation through the crystal. For example, instead of the variation of the relative neutron–crystal velocity, the crystal temperature can be varied or the crystal can be deformed by squeezing. Both actions will cause a change in the crystal interplanar dimensions and so to the shift of the Bragg energy. The crystal movement was chosen due to the convenience of its realization (the above-mentioned accelerated medium effect [18] is negligible in this case). Numerical estimations show that for the quartz crystal plane (110) the Bragg width in the neutron-velocity units is equal to $\Delta v_B \cong 9$ mm/s, i.e., if the crystal velocity changes by 9 mm/s over the time interval of neutron transit through the crystal, the deviation from the Bragg condition will vary by one Bragg width.

The scheme of our experimental setup is shown in Fig. 1. The preselected neutron beam (the beam size is about 3 cm × 1 cm), reflected by the mosaic crystal of pyrolytic graphite (PG) with reflecting plane (002), falls on the monochromator K_1 made from perfect quartz crystal. Reflected by K_1 highly monoenergetic (within Darwin width) neutrons pass through the working crystal K_3 (the size is 5 cm × 5 cm × 10 cm) and then are reflected by the crystal-analyzer K_2. The second PG crystal redirects these reflected neutrons to the detector. The quartz crystals K_1, K_2 and K_3 with the same working reflecting planes (110) were arranged to have their plane orientations in parallel directions. The diffraction angle was close to the right one: $\theta_B = 89^\circ$ ($\lambda \approx 4.9$ Å). Scanning over the Bragg wave length performed by varying temperature difference $T_{21} = T_2 - T_1$ between crystals K_2 and K_1, the temperature T_3 of

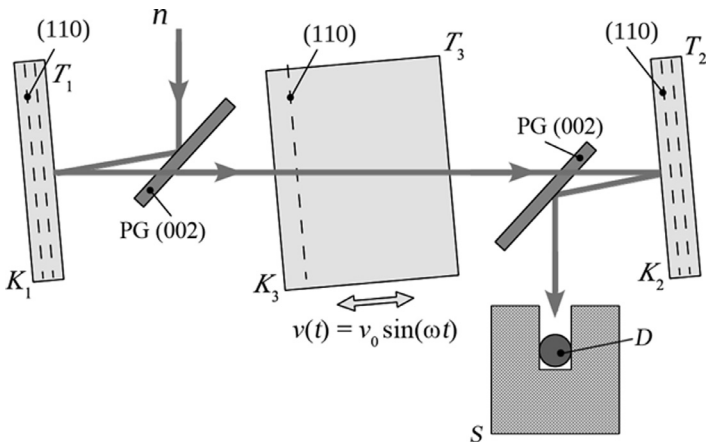

Fig. 1. Scheme of the experimental setup: K_1 is the monochromator; K_2 is the crystal-analyzer; K_3 is the working crystal; PG are the mosaic crystals of pyrolytic graphite; T_1, T_2, T_3 are the crystal temperatures; n is the neutron beam; (002), (110) are the reflecting planes; $v(t)$ is the time-dependent speed of crystal K_3; D is a neutron detector inside a neutron shield S.

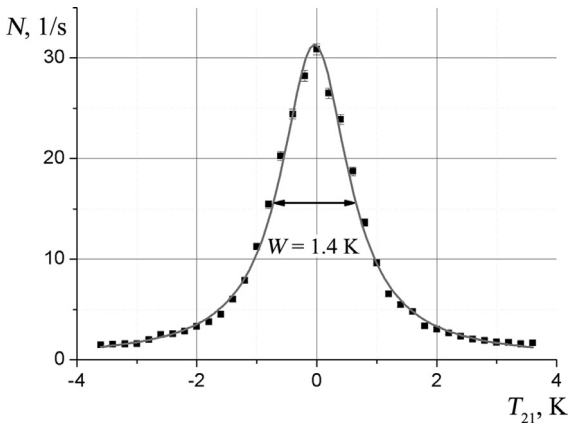

Fig. 2. The experimental (symbols) and the calculated (solid line) two-crystal reflection curves. They reach their maxima when interplanar distances for K_1 and K_2 crystals (see Fig. 1) coincide ($T_{21} = T_2 - T_1 = 0$); N is the neutron intensity. The width W (in Kelvin) corresponds to $\Delta d/d = 1.8 \cdot 10^{-5}$ (in d units of interplanar distance).

the crystal K_3 being a reference one. Example of a scanning curve is shown in Fig. 2, when the crystal K_3 is absent. We have scanned the shape of neutron reflex from the K_1 crystal changing T_{21} and so the relative interplanar distance for the K_2 crystal-analyzer. The width of this convolution scanning curve is close to that calculated (solid line) for two perfect crystals.

There was a possibility to vary the temperature of the crystal K_3 and so its interplanar distance too. Also we could move it in the direction parallel to the reciprocal lattice vector **g** for working plane. To carry out an experiment, the crystal was set in harmonic motion by a piezoelectric motor. The frequency of crystal vibration was $\nu_c = 4.5\,\text{kHz}$ and the period $\tau_c = 222\,\mu\text{s}$. Vibration amplitude reached a value of $0.15\,\mu\text{m}$. The crystal length was $L = 5\,\text{cm}$ and neutron time-of-flight through the crystal was $\tau_n = 62\,\mu\text{s}$ that was about a quarter of the crystal vibration period.

If the speed of the working crystal K_3 depends on time as

$$v(t) = v_0 \cdot \sin \omega\, t, \tag{6}$$

the deviation from the Bragg condition for the neutrons moving through that crystal will also depend on time in the same way

$$\Delta_{\text{B}}(t) = \Delta_{\text{B}_0} + 4\frac{1}{\nu_n}\frac{E_{\text{B}}}{V_g}v(t), \tag{7}$$

where ν_n is the speed of incident neutrons, $\Delta_{B_0}$is the deviation from the Bragg condition for resting crystal at $v(t) = 0$. This deviation Δ_{B_0} is determined by the T_{13} difference of temperatures (interplanar distances) between K_1 and K_3 crystals $T_{13} = T_1 - T_3$. So further we will use this temperature difference T_{13} as a parameter of deviation from the Bragg condition for the neutrons passing the resting K_3 crystal. The relationship between parameters Δ_{B_0} and T_{13} is given by the expression

$$\Delta_{B_0} = 4\frac{E_{\text{B}}}{V_g}\alpha_L\, T_{13}, \tag{8}$$

where $\alpha_L \cong 1.3 \cdot 10^{-5}$ is the linear thermal expansion coefficient for a quartz crystal in the direction perpendicular to crystallographic planes.

The effect of the neutron energy change after passing through the crystal boundaries is determined by variation of the crystal velocity and so the averaged

potential (5) is done during the neutron time-of-flight through the accelerated crystal:

$$\Delta E(t_0) = V_g\left(\frac{\Delta_B(t_2)}{\Delta_B^2(t_2)+1} - \frac{\Delta_B(t_1)}{\Delta_B^2(t_1)+1}\right) = \frac{1-\Delta_{B_0}^2}{(1+\Delta_{B_0}^2)^2}\frac{4E_B}{v_n}\Delta v(t_0), \quad (9)$$

where $\Delta v(t_0) = v(t_0) - v(t_0+\tau_n)$, t_0 is the entry time of neutron into the crystal, τ_n is the neutron time-of-flight through the crystal. Notice once more that the neutron kinetic energy (wave vectors) inside the crystal cannot change because of homogeneity of the averaged crystal potential.

The change (9) of neutron energy (as well as the wavelength) after accelerated crystal results in a shift of the scanning-curve maximum (see Fig. 2). This maximum will be found for some other temperature difference T_{21} of the K_2 and K_1 crystals. Such variations of the scanning curve, depending on temperature and movement of the K_3 crystal, were studied to find how the crystal acceleration effects. Time-of-flight technique was used for this purpose.

The main systematic error of this experiment is associated with the dependence of the neutron transmission through the K_3 crystal on the deviation from the Bragg condition in this crystal, that results in the spectrum distortion for neutrons passed through the crystal. Therefore, the position and shape of the scanning curve can change for neutrons passed even through the resting K_3 crystal, when the acceleration effect is absent. Examples of the neutron intensity distribution over the wave length after such passage through the resting K_3 crystal with different deviations T_{31} from the Bragg condition are shown in Fig. 3. It is evident that both the intensity of the transmitted neutrons and the maximum position of the scanning curve can change in different ways. In particular, for $T_{31} = 0$ K, the neutrons cannot penetrate into the K_3 crystal after reflection from the K_1 crystal. They will be completely reflected (due to the exact Bragg condition) and cannot reach the K_2 crystal. So the latter will reflect only background neutrons. In the other case, for $T_{31} \gg 5$ K, crystal behaves as a homogeneous medium and practically does not distort the spectrum. In an intermediate case, the spectrum will be distorted, because the neutron K_3 crystal reflectivity (and so its transmittance) sharply depends on the neutron wavelength.

However, unlike the sought crystal acceleration effect (9), the curve distortion is determined only by the deviation from the exact Bragg condition at the entry

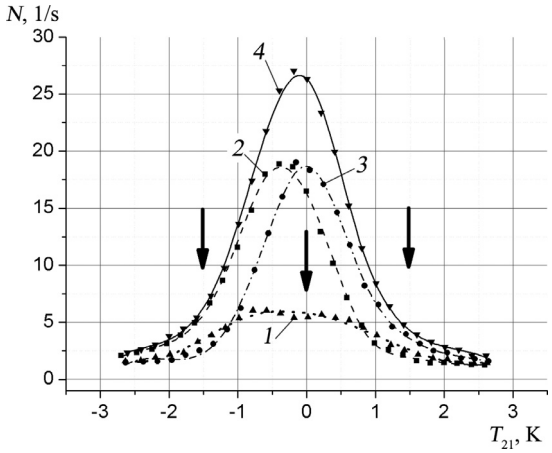

Fig. 3. Two-crystal scanning curves for neutrons passed through immovable working crystal with different deviations T_{31} from the Bragg energy. T_{31}, K: 0 (1), +1.5 (2), –1.5 (3), > 5 (4). The arrows point to exact Bragg positions for K_3 crystal.

time t_0 of neutron to crystal, but not by variation of the deviation during the time-of-flight through the crystal.

So the position $E_s(t_0)$ of the maximum and the maximum intensity $N(t_0)$ of the scanning curve (see Fig. 2) in the absence of the crystal acceleration effect will be some functions of deviation $\Delta_B(t_0)$, depending on the crystal speed $v(t_0)$:

$$E_s(t_0) = F(\Delta_B(t_0)), \quad (10)$$

$$N(t_0) = G(\Delta_B(t_0)). \quad (11)$$

For further consideration and comparison with the experimental results expressions (10) and (11) can be expanded by Taylor series over $v(t_0)$ about the point $v(t_0) = 0$ (i.e., $\Delta_B(t_0) = \Delta_{B_0}$). Taking into account that the crystal speed was significantly less than the typical Bragg widths, it is enough to leave expansion terms up to second order over $v(t_0)$:

$$E_s(t_0) = A + B\cdot v(t_0) + C\cdot v(t_0)^2, \quad (12)$$

$$N(t_0) = N_0 + N_1\cdot v(t_0) + N_2\cdot v(t_0)^2, \quad (13)$$

where A, B, C, N_0, N_1 and N_2 are the free parameters depending on Δ_{B_0} to be found from experiment.

As it follows from (9), the crystal acceleration effect contains a term phase-shifted with respect to the false effect (12) by the value of $\omega\tau_n/2$. This shift is approximately equal to $\pi/4$ for our experimental conditions. Furthermore, the presence of acceleration effect does not change the intensity of the line, but gives its additional shift. Thus, there is a phase shift between the time dependencies of $N_{exp}(t_0) = N(t_0)$ and

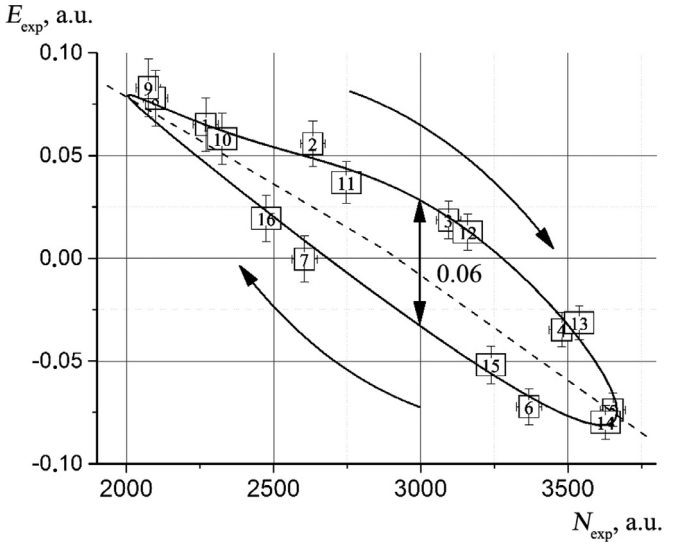

Fig. 4. The plots of the line positions versus its maximum intensities $E_{exp}(N_{exp})$. The initial deviation from the Bragg condition for the working crystal $T_{13} = +1.5$ K. Numbers inside the experimental points correspond to the channel numbers of time spectrum. The solid curve is the result of fitting the experimental data; the dashed line indicates a bijection between the maximum positions and the intensities; curved arrows show the sweep direction over time.

$E_{exp}(t_0) = E_s(t_0) + \Delta E(t_0)$ that represents the crystal acceleration effect.

4. Results and discussion

An example of experimental dependence of the line positions on its maximal intensity $E_{exp}(N_{exp})$ is shown in Fig. 4. In the absence of the acceleration effect a bijection between the maximum positions and the intensities should be observed, shown by a dashed line. The presence of the neutron energy change after passage through the accelerating crystal leads to the dependence $E_{exp}(N_{exp})$ described with a closed curve like Lissajous figure, where the figure square is determined by the crystal acceleration effect. Curved arrows in Fig. 4 show the sweep direction over time. The relation between a line shift in units of the crystal temperature and a change in the neutron energy is given by the following expression:

$$\Delta E = 2E_B \cdot \alpha_L \Delta T. \quad (14)$$

The splitting marked by arrows in Fig. 4 corresponds to $\Delta E_{exp} \cong 5$ neV.

Examples of the time dependencies of the scanning curve maximum position are shown in Fig. 5 for different deviations T_{13} from the Bragg condition. Those are the results of fitting the experimental curves under the assumption that the maximum position is determined by a sum of two effects: see formulae (12) and (9).

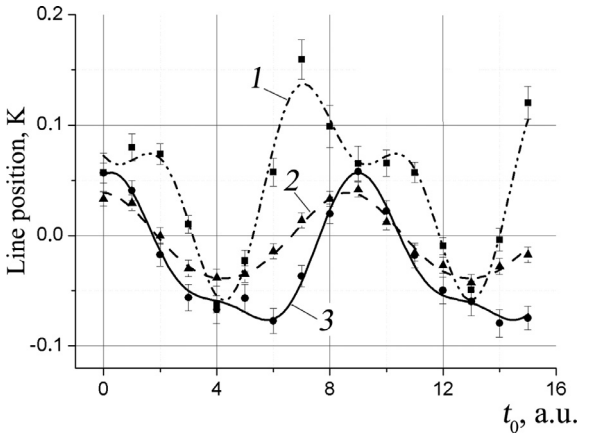

Fig. 5. The experimental dependence of the line position on the entry time t_0 of neutrons into the crystal for various T_{13} – initial deviations from the Bragg condition; T_{31}, K: +1.0 (1), –1.5 (2), –2.5 (3). Horizontal axis t_0 in time-of-flight (TOF) channel units. One channel is equal to 25.6 μs.

Dependence of the maximum value for an energy change (9) due to the acceleration effect on the deviation from the neutron Bragg energy for working crystal (temperature difference T_{13}) is shown in Fig. 6. Measurements were carried out at two different crystal oscillation amplitudes, corresponding to $v_0 \cong 3$ mm/s and $v_0 \cong 1.5$ mm/s (see Eq. (6)). Curves show the results of approximating the experimental points by the theoretical curve (9). Thus, one can see

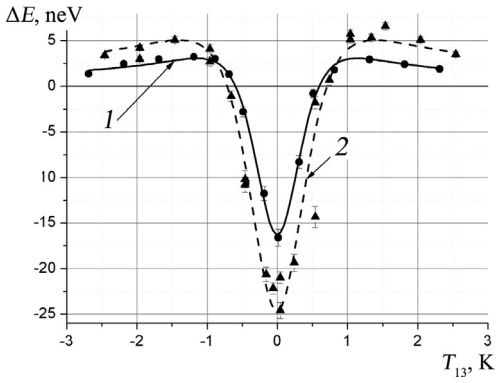

Fig. 6. The experimental (symbols) magnitude of energy variation of a neutron passed through the accelerating crystal as a function of the deviation from the Bragg condition for incident beam, and this function approximation (solid and dashed lines); measurements were carried out at two different crystal oscillation amplitudes, corresponding to $v_0 = 1.5$ mm/s (1) and 3.0 mm/s (2).

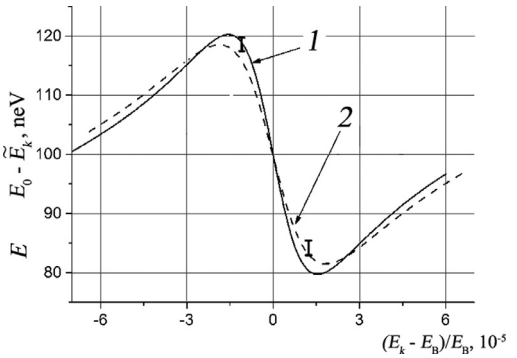

Fig. 7. The behavior of the interaction potential $E_0 - \tilde{E}_k$(see Eq. (5)) of neutrons with the crystal in the vicinity of the Bragg energy. Calculated and reconstructed from Fig. 6 curves coincide in error limits; the curves for different v_0 ($v_0 = 1.5$ mm/s (1) and $v_0 = 3.0$ mm/s (2)) coinside also (vertical bars show the scale of the experimental error).

that the neutron energy change after passage through accelerating crystal can reach ∼20 neV.

The mean potential energy of a neutron–crystal interaction (see Eq. (5)) can be obtained from the experimental dependence shown in Fig. 6, because that is actually a derivative of function (5) (see Eq. (6)). One should take into account that far from the Bragg condition the correction to the mean interaction potential due to the presence of g-harmonic V_g tends to zero (see Eq. (4)), and so neutron refraction will be determined only by the average potential V_0. The result of the interaction potential reconstruction for neutrons moving in a crystal with energies close to the Bragg one is shown in Fig. 7. It is easy to see that the relative change of the neutron energy by several units of 10^{-5} leads to the variation of the interaction neutron–crystal potential by $\pm 20\%$.

5. Summary

The features of refraction of a neutron wave moving in a crystal close to the Bragg condition has been studied. The energy dependence of refractive index was shown to exhibit an evident resonance shape in the vicinity of the Bragg energy with the corresponding Bragg (Darwin) width (for thermal and cold neutrons $\Delta E/E \cong 10^{-5}$). The variation of the interaction potential of the neutron with the crystal in this energy range can reach about $\pm 20\%$.

The resonance behaviour of the neutron–crystal interaction potential results in one more new phenomenon. That is the neutron acceleration, which is found experimentally for neutrons passed through the accelerating perfect crystal for neutron energies close to the Bragg one. The effect arises due to a change in the parameter of deviation from the exact Bragg condition during the neutron time-of-flight through the accelerating crystal. As a result the refraction index for neutron changes as well and so does the velocity of the outgoing neutron.

This crystal acceleration effect has been observed for the first time. This phenomenon should be taken into account in precision neutron optical experiments such as mentioned above, because the neutron refraction index is determined not only by the averaged crystal potential, but also by its harmonics, which have the same order of value as the average potential itself.

Acknowledgment

The authors are thankful to the staff of the WWR-M reactor (Petersburg Nuclear Physics Institute, Gatchina, Russian Federation) for the efforts to maintain the performance of this apparatus.

This work was supported by the Ministry of Science and Education of the Russian Federation (Program 3.329.2014/K).

References

[1] Yu.V. Petrov, Possibility of investigating the levels of the compound nucleus produced by interaction between slow neutrons and isomers, Sov. Phys. J. Exp. Theor. Phys. 10 (4) (1960) 833–834.

[2] I.A. Kondurov, E.M. Korotkikh, Yu.V. Petrov, Acceleration of thermal neutrons by 152mEu isomeric nuclei, J. Exp. Theor. Phys. Lett. 31 (4) (1980) 232–235.

[3] I.A. Kondurov, E.M. Korotkikh, Yu.V. Petrov, G.I. Shulyak, Acceleration of thermal neutrons by isomeric nuclei (180Hf m), Phys. Lett. B 106 (5) (1981) 383–385.
[4] Yu.V. Petrov, A.I. Shlyalchter, The cross section of inelastic neutron acceleration for indium isomers, Nucl. Phys. A 292 (1–2) (1977) 88–92.
[5] Yu.V. Petrov, Multiple acceleration of neutrons in an inversely populated medium, Sov. Phys. J. Exp. Theor. Phys. 36 (3) (1973) 395–398.
[6] A.B. Laptev, G.A. Petrov, Yu.S. Pleva, M.A. Yamshikov, Acceleration of thermal neutrons in scattering by vibrationally excited nitrogen molecules, Sov. J. Nucl. Phys. 49 (2) (1989) 204–207.
[7] H. Weinfurter, G. Badurek, H. Rauch, D. Schwahn, Inelastic action of a gradient radio-frequency neutron spin flipper, Z. Phys. B: Condens. Matter 72 (2) (1988) 195–201.
[8] L. Niel, H. Rauch, Acceleration, deceleration and monochromatization of neutrons in time dependent magnetic fields, Z. Phys. B: Condens. Matter 74 (1) (1989) 133–139.
[9] V.V. Voronin, Yu.V. Borisov, A.V. Ivanyuta, et al., Observation of small changes in the energy of a neutron in an alternating magnetic field, J. Exp. Theor. Phys. Lett. 96 (10) (2012) 613–615.
[10] L.A. Rivlin, Laser acceleration of neutrons (physical foundations), Quantum Electron. 40 (5) (2010) 460–463.
[11] A.V. Antonov, D.E. Vul', M.V. Kazarnovskii, Possible method of obtaining ultracoldneutrons by reflection from moving mirrors, J. Exp. Theor. Phys. Lett. 9 (5) (1969) 180–183.
[12] A.Z. Andreev, A.G. Glushkov, P. Geltenbort, et al., Ultracold neutron cooling upon reflection from a moving wall, Tech. Phys. Lett. 39 (4) (2013) 370–373.
[13] T.W. Dombeck, J.W. Lynn, S.A. Werner, et al., Production of ultracold neutrons using Doppler-shifted Bragg scattering and an intense pulsed neutron spallation source, Nucl. Instrum. Methods A 165 (2) (1979) 139–155.
[14] S. Mayer, H. Rauch, P. Geltenbort, et al., New aspects for high-intensity neutron beam production, Nucl. Instrum. Methods A 608 (3) (2009) 434–439.
[15] F.V. Kowalski, Interaction of neutrons with accelerating matter: test of the equivalence principle, Phys. Lett. A 182 (1-2) (1993) 335–340.
[16] V.G. Nosov, A.I. Frank, Interaction of slow-neutrons with moving matter, Phys. At. Nucl. 61 (4) (1998) 613–623.
[17] A.I. Frank, P. Geltenbort, G.V. Kulin, et al., Effect of accelerating matter in neutron optics, J. Exp. Theor. Phys. Lett. 84 (7) (2006) 363–367.
[18] A.I. Frank, P. Geltenbort, M. Jentschel, et al., Effect of accelerated matter in neutron optics, Phys. At. Nucl. 71 (10) (2008) 1656–1674.
[19] A.I. Frank, P. Geltenbort, M. Jentschel, et al., New experiment on the observation of the effect of accelerating matter in neutron optics, J. Exp. Theor. Phys. Lett. 93 (7) (2011) 361–365.
[20] A.I. Frank, V.A. Naumov, Interaction of waves with a birefringent medium moving with acceleration, Phys. At. Nucl. 76 (12) (2013) 1423–1433.
[21] V.V. Voronin, Ya.A. Berdnikov, A.Ya. Berdnikov, et al., Dispersion of the refractive index of a neutron in a crystal, J. Exp. Theor. Phys. Lett. 100 (8) (2014) 497–502.
[22] P. Hirsch, A. Howie, R. Nicholson, et al., Electron Microscopy of Thin Crystals, Butterworths, London, 1965.
[23] V.L. Alexeev, V.V. Fedorov, E.G. Lapin, et al., Observation of a strong interplanar electric field in a dynamical diffraction of a polarized neutron, Nucl. Instrum. Methods A 284 (1) (1989) 181–183.
[24] V.L. Alexeev, V.V. Voronin, E.G. Lapin, et al., Measurement of the strong intracrystalline electric field in the Schwinger interaction with diffracted neutrons, Sov. Phys.: J. Exp. Theor. Phys. 69 (6) (1989) 1083–1085.
[25] V.V. Fedorov, I.A. Kuznetsov, E.G. Lapin, et al., Neutron spin optics in noncentrosymmetric crystals as a new way for nEDM search, Nucl. Instrum. Methods B 252 (1) (2006) 131–135.
[26] V.V. Fedorov, V.V. Voronin, Neutron diffraction and optics in noncentrosymmetric crystals. New feasibility of a search for neutron EDM, Nucl. Instrum. Methods B 201 (1) (2003) 230–242.
[27] V.V. Fedorov, V.V. Voronin, E.G. Lapin. On the search for neutron EDM using Laue diffraction by a crystal without a center of symmetry. Preprint LNPI-1644, Leningrad, 1990.
[28] V.V. Fedorov, On the possibility for neutron EDM search using diffraction by crystal without a center of symmetry, in: Proceedings of XXVI LNPI Winter School, Leningrad, 1991, pp. 65–118.
[29] V.V. Fedorov, V.V. Voronin, E.G. Lapin, On the search for neutron EDM using Laue diffraction by a crystal without a centre of symmetry, J. Phys. G 18 (7) (1992) 1133–1148.
[30] V.V. Fedorov, M. Jentschel, I.A. Kuznetsov, et al., Measurement of the neutron electric dipole moment by crystal diffraction, Nucl. Instrum. Methods A 611 (2-3) (2009) 124–128.
[31] V.V. Fedorov, M. Jentschel, I.A. Kuznetsov, et al., Measurement of the neutron electric dipole moment via spin rotation in a non-centrosymmetric crystal, Phys. Lett. B 694 (1) (2010) 22–25.
[32] V.V. Voronin, V.V. Fedorov, I.A. Kuznetsov, Neutron diffraction constraint on spin-dependent short range interaction, J. Exp. Theor. Phys. Lett. 90 (1) (2009) 5–7.
[33] V.V. Voronin, Yu.V. Borisov, A.V. Ivanyuta, et al., Anomalous behavior of the dispersion of a neutron transmitting through a crystal at nearly Bragg energies, J. Exp. Theor. Phys. Lett. 96 (10) (2012) 609–612.
[34] V.V. Fedorov, V.V. Voronin, New possibilities for neutron EDM search by polarization method using diffraction in the crystal without a centre of symmetry, in: Proceedings of XXVI PNPI Winter School, St. Petersburg, 1996, pp. 123–164.